

# Numerical Solution of the Problem of Ignition of a Combustible Liquid by a Single Hot Particle

G. V. Kuznetsov,<sup>1</sup> and P. A. Strizhak<sup>1</sup>

UDC 536.468

Translated from *Fizika Goreniya i Vzryva*, Vol. 45, No. 5, pp. 42–50, September–October, 2009.  
Original article submitted November 21, 2007; revision submitted December 30, 2008.

The problem of ignition of a typical combustible liquid by a single metal particle heated to high temperatures is solved numerically using a gas-phase model of ignition taking into account thermal conductivity, liquid vaporization, diffusion and convection of fuel vapor in air, crystallization of the particle, formation of a vapor gap between the particle and liquid, temperature dependence of the thermal characteristics of interacting substances, and air humidity. The scales of the effects of the initial temperature and particle size and shape on the delay of the examined process are determined. The limiting values for ignition initiation are found for the characteristic parameters of the ignition source (initial temperature and size) and air humidity.

**Key words:** ignition, liquid combustible substance, hot metal particle, numerical study, ignition delay.

## INTRODUCTION

The heating, vaporization, ignition, and combustion of liquid substances with various methods of energy delivery (massive heated bodies, hot gases, single heated particles of various physical natures, etc.) are very important processes in many applications [1–6], in particular, power engineering and chemical and oil refining industries.

Many interactions of liquids with various heat sources have been studied by numerical modeling [2, 3, 6]. However, the models used for this purpose do not take into account a number of factors that can have a significant influence on the modeled processes. Thus, the ignition and combustion of liquids are traditionally studied using kinetic ignition models of liquid drops [7, 8]. However, the well-known kinetic ignition models are unsuitable for effective studies of liquid ignition and combustion in tanks or in the open air because these models ignore the specificity of heat and mass transfer during liquid ignition. It has been found [8, 9] that the ignition and combustion of various substances are determined mainly by the longer physical processes of heat and mass transfer and not by fast chemical reactions.

Six mechanisms of energy delivery for solid ignition that are also true for liquid ignition are described in [10]. Among them, the least studied is heating by single hot particles formed during cutting, welding or friction of metals and by nonmetallic particles formed during man-made events (for example, fires and explosions). Interacting with liquids, such particles act as sources of local ignition [6, 10].

The purpose of the present work was to perform a numerical study of the ignition of a combustible liquid by a metal particle using a gas-phase ignition model that takes into account heat and mass transfer, diffusion and convection of fuel vapor in air, liquid vaporization, kinetics of vaporization and ignition of the combustible liquid, crystallization of the heating source, formation of a vapor gap between the particle and liquid, temperature dependence of the thermal characteristics of the interacting substances, and air humidity.

## FORMULATION OF THE PROBLEM

A gas-phase model of ignition of a combustible liquid (gasoline) by a single metal (steel) particle heated to high temperatures was considered. The ignition source was a molten metal particle covered by a shell of crys-

<sup>1</sup>Tomsk Polytechnical University, Tomsk 634050; pavel-strizhak@yandex.ru.

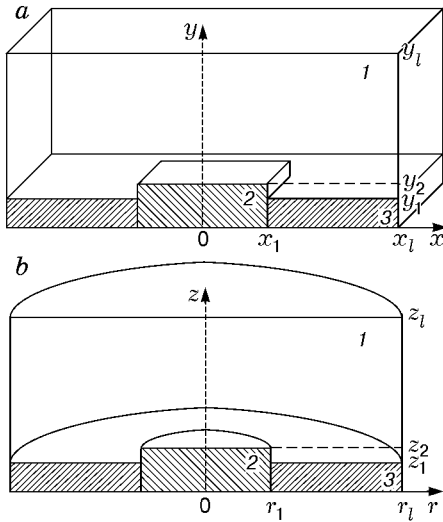


**Fig. 1.** Geometrical model of the examined process in Cartesian coordinates (a) and cylindrical coordinates (b): 1) air; 2) particle; 3) liquid.

tallized material. To analyze the effect of the particle shape on the rate of the examined process, we solved the problem in Cartesian system (Fig. 1a) and cylindrical coordinate systems (Fig. 1b), whose origin coincided with the symmetry axis of the particle. The results of solution of this problem in a simpler formulation in Cartesian coordinates are presented in [6]. Below we give a solution for cylindrical coordinates.

In the case of a particle having the shape of a cylinder (disk), the contact surface between the particle and the liquid can be modeled more accurately. In the liquid, we distinguished a cylindrical region whose radius  $r_l$  was much larger than the size of the cylindrical particle  $r_{ch} = r_1$ . The case of the particle falling into the liquid fuel film on the surface of a solid was considered. The particle was not completely immersed in the liquid substance (particle height  $z_{ch} = z_2$  is larger than the height of the layer of the combustible liquid film  $z_1$ ).

The following sequence of stages of the process was assumed. The particle heated to high temperatures fell on the surface of the combustible liquid and dipped in it (Fig. 2a). Due to the heat accumulated in the particle and released during metal crystallization, the liquid is heated and vaporized. This leads to the formation of a vapor gap between the particle and liquid (Fig. 2b). The fuel vapor moves from the vaporization surface and mixes with air. A vapor-gas mixture forms, which is ignited upon reaching certain temperatures and fuel concentrations.

The numerical study was performed under the following assumptions:

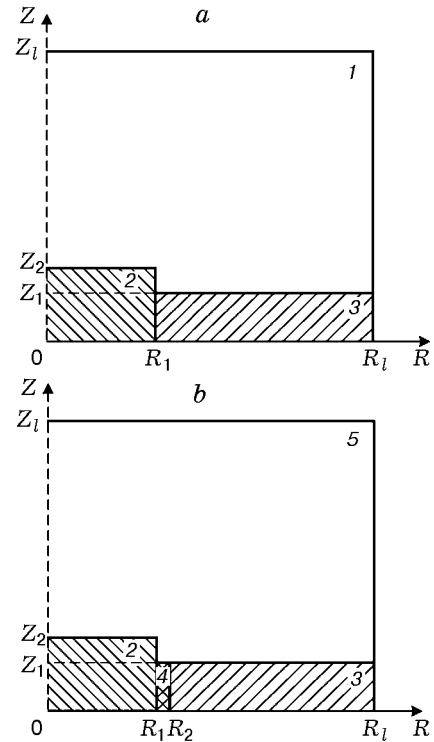


**Fig. 2.** Diagram of the domain of solution of the problem at the initial ( $\tau = 0$ ) time (a) and at  $0 < \tau < \tau_d$  (b): 1) air; 2) particle; 3) liquid; 4) layer fuel vapor; 5) vapor-gas mixture.

1) Vaporization of the liquid results in one substance with known characteristics. This approach is traditionally used in solutions of ignition problems for liquid and solid condensed substances [9];

2) Combustion of the liquid was ignored; the liquid film was assumed to occupy a large area;

3) Convective flows in the liquid due to its heating can be ignored as a first approximation because theoretical and experimental studies of the ignition of drops of typical liquid fuels by massive heated solids [7] have shown that the characteristic convection time in a heated fuel is several times larger than the ignition delay.

Taking into account the features of the examined ignition process related to the cooling of a heating source of small size which has a finite energy resource, we adopted the following ignition conditions [9]:

1) the heat released in the chemical reaction of fuel vapor with an oxidizer is larger than the heat transferred from the particle to the combustible liquid and vapor-gas mixture;

2) the temperature of the vapor-gas mixture exceeds the initial temperature of the particle.

## MATHEMATICAL FORMULATION

The system of nonlinear nonstationary differential equations for the examined gas-phase ignition model (see Fig. 2b) in the dimensionless variables has the following form ( $0 < \tau < \tau_d$ ): for

$$R_1 < R < R_2, \quad 0 < Z < Z_1;$$

$$R_1 < R < R_l, \quad Z_1 < Z < Z_2;$$

$$0 < R < R_l, \quad Z_2 < Z < Z_l,$$

Poisson's equation is

$$\frac{\partial^2 \Psi}{\partial R^2} + \frac{1}{R} \frac{\partial \Psi}{\partial R} + \frac{\partial^2 \Psi}{\partial Z^2} = \Omega, \quad (1)$$

the equation of motion for the fuel vapor-air mixture is

$$\begin{aligned} & \frac{1}{\text{Sh}} \frac{\partial \Omega}{\partial \tau} + U \frac{\partial \Omega}{\partial R} + V \frac{\partial \Omega}{\partial Z} \\ & = \frac{1}{\text{Re}_5} \left[ \frac{\partial^2 \Omega}{\partial R^2} + \frac{1}{R} \frac{\partial \Omega}{\partial R} + \frac{\partial^2 \Omega}{\partial Z^2} \right] + \frac{\text{Gr}_5}{\text{Re}_5^2} \frac{\partial \Theta}{\partial Z}, \end{aligned} \quad (2)$$

the energy equation is

$$\begin{aligned} & \frac{1}{\text{Sh}} \frac{\partial \Theta_5}{\partial \tau} + U \frac{\partial \Theta_5}{\partial R} + V \frac{\partial \Theta_5}{\partial Z} \\ & = \frac{1}{\text{Re}_5 \text{Pr}_5} \left[ \frac{\partial^2 \Theta_5}{\partial R^2} + \frac{1}{R} \frac{\partial \Theta_5}{\partial R} + \frac{\partial^2 \Theta_5}{\partial Z^2} \right] + \text{Sr}_1, \end{aligned} \quad (3)$$

the equation of diffusion of fuel vapor in air is

$$\begin{aligned} & \frac{1}{\text{Sh}} \frac{\partial C_{m,g}}{\partial \tau} + U \frac{\partial C_{m,g}}{\partial R} + V \frac{\partial C_{m,g}}{\partial Z} = \frac{1}{\text{Re}_4 \text{Sc}_4} \\ & \times \left[ \frac{\partial^2 C_{m,g}}{\partial R^2} + \frac{1}{R} \frac{\partial C_{m,g}}{\partial R} + \frac{\partial^2 C_{m,g}}{\partial Z^2} \right] + \text{Sr}_2, \end{aligned} \quad (4)$$

the equation of diffusion of water vapor in air is

$$\begin{aligned} & \frac{1}{\text{Sh}} \frac{\partial C_{m,w}}{\partial \tau} + U \frac{\partial C_{m,w}}{\partial R} + V \frac{\partial C_{m,w}}{\partial Z} = \frac{1}{\text{Re}_{12} \text{Sc}_{12}} \\ & \times \left[ \frac{\partial^2 C_{m,w}}{\partial R^2} + \frac{1}{R} \frac{\partial C_{m,w}}{\partial R} + \frac{\partial^2 C_{m,w}}{\partial Z^2} \right], \end{aligned} \quad (5)$$

and the equation of balance is

$$C_{m,g} + C_{m,\text{ox}} + C_{m,w} = 1; \quad (6)$$

for  $0 < R < R_1$  and  $0 < Z < Z_2$ , the heat-conduction equation for the particle is

$$\frac{1}{\text{Fo}_2} \frac{\partial \Theta_2}{\partial \tau} = \frac{\partial^2 \Theta_2}{\partial R^2} + \frac{1}{R} \frac{\partial \Theta_2}{\partial R} + \frac{\partial^2 \Theta_2}{\partial Z^2} + \text{Sr}_3; \quad (7)$$

for  $R_2 < R < R_l$  and  $0 < Z < Z_1$ , the heat-conduction equation for the liquid is

$$\frac{1}{\text{Fo}_3} \frac{\partial \Theta_3}{\partial \tau} = \frac{\partial^2 \Theta_3}{\partial R^2} + \frac{1}{R} \frac{\partial \Theta_3}{\partial R} + \frac{\partial^2 \Theta_3}{\partial Z^2}. \quad (8)$$

The dimensionless complexes are given by

$$\text{Gr}_5 = \frac{\beta g z_l^3 \Delta T \rho_5(T)^2}{\mu_5(T)^2},$$

$$\text{Fo}_2 = \frac{\lambda_2(T) t_m}{\rho_2(T) c_2(T) z_l^2},$$

$$\text{Fo}_3 = \frac{\lambda_3(T) t_m}{\rho_3(T) c_3(T) z_l^2},$$

$$\text{Pr}_5 = \frac{\mu_5(T) c_5(T)}{\lambda_5(T)},$$

$$\text{Re}_i = \frac{2v_m z_l \rho_i(T)}{\mu_i(T)}, \quad i = 4, 5, 12,$$

$$\text{Sh} = \frac{v_m t_m}{z_l},$$

$$\text{Sc}_i = \frac{\mu_i(T)}{D_i(T) \rho_i(T)}, \quad i = 4, 12,$$

$$\text{Sr}_1 = \frac{Q_{\text{ox}} W_{\text{ox}} z_l}{\rho_5(T) c_5(T) \Delta T v_m},$$

$$\text{Sr}_2 = \frac{z_l W_{\text{ox}}}{\rho_4(T) v_m},$$

$$\text{Sr}_3 = \frac{Q_{\text{cr}} W_{\text{cr}} z_l}{z_{\text{ch}} \Delta T \lambda_2(T)}.$$

Here  $\tau$  is dimensionless time,  $\tau_d$  is the dimensionless ignition delay ( $\tau_d = t_d/t_m$ ),  $t$  [sec] is the time,  $t_d$  [sec] is the ignition delay,  $t_m$  is the time scale,  $R$  and  $Z$  are the dimensionless coordinates of the cylindrical coordinate system which correspond to the dimensional coordinates  $r$  and  $z$ , respectively,  $\Psi$  is a dimensionless analog of the stream function,  $\Omega$  is a dimensionless analog of the vorticity vector,  $\text{Sh}$  is the Strouhal number,  $U$  and  $V$  are the dimensionless components of the fuel vapor in projection onto the  $r$  and  $z$  axes,  $\text{Re}$  is the Reynolds number,  $\text{Gr}$  is the Grashof number,  $z_l$  [m] is the characteristic size of the solution domain in projection onto the  $z$  axis,  $\Theta$  is the dimensionless temperature ( $\Theta = T/T_m$ ),  $T$  [K] is the temperature,  $T_m$  is the temperature scale,  $\Delta T = T_m - T_0$ ,  $T_0$  [K] is the initial temperature of the liquid and air,  $g$  [m/sec<sup>2</sup>] is the acceleration due to gravity,  $\beta$  [K<sup>-1</sup>] is the volumetric-expansion coefficient,  $\mu$  [kg/(m · sec)] is the dynamic viscosity,  $\text{Pr}$  is the Prandtl number,  $\text{Sr}_1$ ,  $\text{Sr}_2$ , and  $\text{Sr}_3$  are the dimensionless complexes,  $\rho$  [kg/m<sup>3</sup>] is the density,  $c$  [J/(kg · K)] is the specific heat capacity,  $\lambda$  [W/(m · K)] is the thermal conductivity,  $Q_{\text{ox}}$  [MJ/kg] is the thermal effect of fuel vapor oxidation in air,  $W_{\text{ox}}$  [kg/(m<sup>3</sup> · sec)] is the mass rate of fuel vapor oxidation in air,  $v_m$  [m/sec] is the scale of the fuel vapor convection velocity,  $C_{m,g}$  is the mass concentration of the liquid fuel vapor in the vapor-gas mixture,  $\text{Sc}$  is the Schmidt number,  $C_{m,w}$  is the mass concentration of water vapor in the vapor-gas mixture,  $C_{m,\text{ox}}$  is

the mass concentration of the oxidizer in the vapor–gas mixture,  $D$  [m<sup>2</sup>/sec] is the fuel vapor diffusion coefficient in air,  $Q_{cr}$  [kJ/kg] is the thermal effect of crystallization of the particle material,  $W_{cr}$  [kg/(m<sup>2</sup>·sec)] is the mass rate of crystallization,  $Fo$  is the Fourier number; the subscript 1 corresponds to humid air, 11 to dry air, 12 to water vapor, 2 to the particle, 3 to the combustible liquid, 4 to the combustible vapor, and 5 to the vapor–gas mixture.

The volume fractions of the components of the vapor–gas mixture were calculated from their mass concentrations:

$$\varphi_{11} = \frac{\frac{C_{m,ox}}{\rho_{11}(T)}}{\frac{C_{m,ox}}{\rho_{11}(T)} + \frac{C_{m,w}}{\rho_{12}(T)} + \frac{C_{m,g}}{\rho_4(T)}},$$

$$\varphi_{12} = \frac{\frac{C_{m,w}}{\rho_{12}(T)}}{\frac{C_{m,ox}}{\rho_{11}(T)} + \frac{C_{m,w}}{\rho_{12}(T)} + \frac{C_{m,g}}{\rho_4(T)}},$$

$$\varphi_{11} + \varphi_{12} + \varphi_4 = 1.$$

The thermal characteristics of the vapor–gas mixture as a heterogeneous system consisting of fuel vapor, water vapor, and air were calculated by the formulas

$$\lambda_5(T) = \lambda_{11}(T)\varphi_{11} + \lambda_{12}(T)\varphi_{12} + \lambda_4(T)\varphi_4,$$

$$c_5(T) = c_{11}(T)\varphi_{11} + c_{12}(T)\varphi_{12} + c_4(T)\varphi_4,$$

$$\rho_5(T) = \rho_{11}(T)\varphi_{11} + \rho_{12}(T)\varphi_{12} + \rho_4(T)\varphi_4.$$

The initial conditions (see Fig. 2a) ( $\tau = 0$ ) were as follows:  $\Theta = \Theta_{ch}$  at  $0 < R < R_1$  and  $0 < Z < Z_2$ ;  $\Theta = \Theta_0$  at  $R_1 < R < R_l$  and  $0 < Z < Z_1$ ;  $\Omega = 0$ ,  $\Psi = 0$ ,  $C_{m,g} = C_{m,g0}$ ,  $C_{m,w} = C_{m,w0}$ , and  $\Theta = \Theta_0$  at  $R_1 < R < R_l$  and  $Z_1 < Z < Z_2$ ;  $0 < R < R_l$  and  $Z_2 < Z < Z_l$ . Here  $C_{m,g0}$  and  $C_{m,w0}$  are the initial mass concentrations of fuel vapor and water in air,  $\Theta_{ch}$  is the dimensionless initial temperature of the particle, and  $\Theta_0$  is the dimensionless initial temperature of the liquid and air.

The boundary conditions (see Fig. 2b) ( $0 < \tau < \tau_d$ ) were taken by analogy with [6]: the boundary conditions of the fourth kind for the energy and heat-conduction equations, the condition of zero gradients of the corresponding functions for the diffusion, motion, and Poisson's equations were taking at the interfaces between the particle and vapor fuel ( $R = R_1$  and  $0 < Z < Z_1$ ) and interfaces between the particle and vapor–gas mixture ( $R = R_1$  and  $Z_1 < Z < Z_2$ ;  $Z = Z_2$  and  $0 < R < R_1$ ); boundary conditions of the fourth kind taking into account liquid vaporization for the energy equation, boundary conditions of the second kind

for the diffusion, motion, and Poisson's equations were taking at the interface between the liquid and vapor fuel ( $R = R_2$  and  $0 < Z < Z_1$ ) and interface between the vapor–gas mixture and the liquid ( $Z = Z_1$  and  $R_2 < R < R_l$ ), and zero gradients of the corresponding functions for all equations were taking on the symmetry axis and the interfaces ( $Z = 0$ ,  $Z = Z_l$ , and  $0 < R < R_l$ ;  $R = R_l$  and  $0 < Z < Z_l$ ;  $Z = Z_1$  and  $R_1 < R < R_2$ ).

The variables were made dimensionless using  $z_l$  [m] as the linear scale,  $t_m$  [sec] as the time scale,  $T_m$  [K] as the temperature scale, and  $v_m$  [km/sec] as the velocity scale.

The fuel vapor convection velocity in the gas region near the boundary of liquid vaporization was given by the formula [11]

$$v_m = \sqrt{g\beta\Delta T z_l}.$$

The mass oxidation rate of the combustible liquid vapor in air was calculated using the expression [12]

$$W_{ox} = k_0 C_{m,g}^{m_1} C_{m,ox}^{m_2} \rho_5(T) \exp\left(-\frac{E}{RT_5}\right),$$

where  $k_0$  [sec<sup>-1</sup>] is the preexponent,  $m_1$  and  $m_2$  are constants,  $E$  [kJ/mole] is the activation energy, and  $R$  [J/(mole·K)] is the universal gas constant.

The mass rate of gasoline vapor formation was determined from the relation [13]

$$W_{vap} = \frac{A(p^n - p)}{\sqrt{2\pi RT_p/M}},$$

where  $A$  is the accommodation coefficient,  $A = 35/(p^n)^{0.56}$  [14],  $p^n$  [N/m<sup>2</sup>] is the saturation vapor pressure of the liquid substance,  $p$  [N/m<sup>2</sup>] is the pressure vapor above the liquid surface,  $M$  [kg/mole] is the molecular weight of the liquid substance, and  $T_p$  [K] is the liquid surface temperature.

The mass rate of crystallization of the heating source was calculated by the formula

$$W_{cr} = v_{cr}\rho_2(T),$$

where  $v_{cr}$  [m/sec] is the linear rate of crystallization of the heating source.

The linear rate of crystallization of the heating source, as the rate of motion of the isotherm  $\Theta = \Theta_{cr}$ , was determined by numerical solution in each time step using the expression

$$v_{cr} = \frac{\delta(r, z, t + \Delta t) - \delta(r, z, t)}{\Delta t},$$

where  $\delta(r, z, t + \Delta t)$  and  $\delta(r, z, t)$  [m] are the distances from the lower end of the particle to the crystallization front at the times  $t + \Delta t$  and  $t$ , respectively,  $\Delta t$  [sec] is the time step, and  $\Theta_{cr}$  is the dimensionless melting point of the particle material.

## METHOD OF SOLUTION

System (1)–(8) with the corresponding initial and boundary conditions was solved using a finite difference method [15]. Difference analogs of the differential equations were solved by a locally-one-dimensional method [15]. An iterative method [16] and a marching method with an implicit four-point scheme [15] were employed to solve the one-dimensional difference equations. To increase the accuracy and reduce the volume of calculations, we used a nonuniform time step ( $10^{-4}$ – $10^{-6}$  sec) and an irregular spatial grid (200–400 nodes on each of the coordinates). The reliability of the results was determined by testing the conservatism of the difference scheme as is described in [17].

The characteristic size of the vapor gap between the particle and liquid ( $R_{p,z} = R_2 - R_1$ ) was refined in each time step. The pressure of the fuel vapor rising along the lateral sides of the particle ( $p_p$ ) and the liquid pressure in the gap ( $p_l$ ) were calculated. The pressure  $p_l$  as a first approximation can be set equal to the pressure of a liquid column whose height is equal to the thickness of the liquid film  $Z_l$ .

The pressures  $p_p$  and  $p_l$  were calculated by the formulas

$$p_p = \frac{\rho_4 v^2}{2}, \quad p_l = \rho_3 z_1 g,$$

where  $v$  [km/sec] is the fuel vapor velocity in the gap in projection onto the  $z$  axis.

If  $p_p = p_l$ , the quantity  $R_{p,z}$  did not change. In the next iteration, quantity  $R_{p,z}$  was decreased by a finite value for  $p_l > p_p$  and increased for  $p_l < p_p$ . The iterations were continued until the equality  $p_p = p_l$  was reached.

## RESULTS AND DISCUSSION

The following characteristics of the interacting substances were assumed [18–21]:  $\Theta_0 = 0.3$ ,  $\Theta_{ch} = 1$ ,  $Q_{ox} = 45$  MJ/kg,  $E = 130$  kJ/mole,  $k_0 = 7 \cdot 10^6$  sec $^{-1}$ ,  $M = 100$  kg/kmole,  $\Theta_{cr} = 1.4$ , and  $Q_{cr} = 205$  kJ/kg. The thermal characteristics of gasoline, its vapor, air, water vapor, and steel particle as functions of temperature are given in [19–21]. Illustrations of the results of numerical studies are given for  $C_{m,g0} = 0$ ,  $C_{m,w0} = 0$ ,  $z_l = 20 \cdot 10^{-3}$  m,  $r_l = 10 \cdot 10^{-3}$  m,  $z_1 = 1 \cdot 10^{-3}$  m,  $z_{ch} = 1.4 \cdot 10^{-3}$  m,  $r_{ch} = 2 \cdot 10^{-3}$  m,  $t_m = 5$  sec, and  $T_m = 1000$  K.

The dependence of the ignition delay on the initial temperature of the hot particle (Table 1) was found. An analysis of the results shows that, as the initial particle temperature  $\Theta_{ch}$  increases, the ignition delay  $\tau_d$  de-

TABLE 1

Ignition Delay in the  
Steel Particle–Gasoline–Air System versus  
Initial Particle Temperature  $\Theta_{ch}$   
for  $R_{ch} = 0.1$  and  $Z_{ch} = 0.07$

$\Theta_{ch}$	$\tau_d$
1.500	0.008
1.400	0.017
1.300	0.026
1.200	0.037
1.100	0.058
1.000	0.095
0.900	0.182
0.800	0.343
0.750	No ignition

creases. This is due to an increase in the heat content of the heating source with increasing  $\Theta_{ch}$  with the other parameters of the process being unchanged. It should be noted that the numerical values  $\tau_d$  for  $\Theta_{ch} = 1.5$  and 0.8 differ by several orders of magnitude. This is due to a change in the location of the ignition zone of the vapor–gas mixture relative to the particle with increasing  $\Theta_{ch}$ .

The numerical analysis shows that, for a particle with characteristic sizes  $R_{ch} = 0.1$  and  $Z_{ch} = 0.07$  for  $\Theta_{ch} < 1.3$ , ignition occurs near the symmetry axis in the gas region above the particle (Figs. 3 and 4). This can be explained by the fact that vaporization of the liquid leads to the formation of a vapor–gas mixture near the liquid surface with a high fuel vapor content but with insufficient temperature for ignition. The vapor flows are additionally heated due to the energy of the particle. At the interface with the air, the particle temperature decreases slightly from the moment of fall on the liquid surface, unlike at the interface with the liquid (Fig. 4). As a result, the air above the particle and then the vapor–gas mixture are heated more strongly. This leads to an increase in both the temperature of the vapor–gas mixture and the fuel vapor concentration in the gas region above the particle.

However, at high temperatures ( $\Theta_{ch} \geq 1.3$ ), the energy of the heated particle is sufficient for ignition of the vapor–gas mixture in immediate proximity to the vaporization boundary. Therefore, at  $\Theta_{ch} \geq 1.3$ , ignition occurs near the lateral surfaces of the particle and not above it, as is shown in Figs. 3 and 4.

Table 2 gives ignition delays versus the characteristic sizes  $H_{ch}$ ,  $L_{ch}$ ,  $R_{ch}$ , and  $Z_{ch}$  (dimensionless analogs  $h_{ch} = x_1$ ,  $l_{ch} = y_2$ ,  $r_{ch} = r_1$ , and  $z_{ch} = z_2$ ) for particles having the shape of a parallelepiped and a cylin-

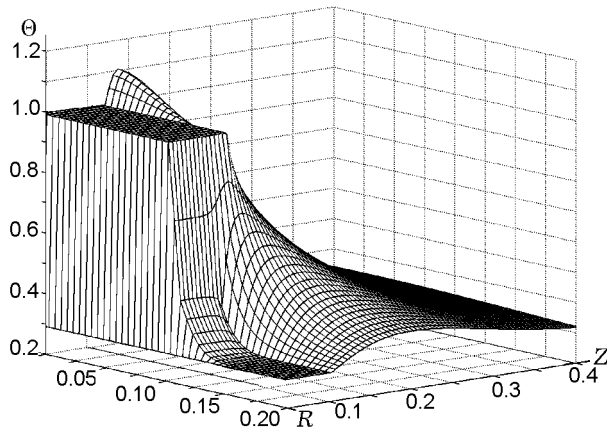


Fig. 3. Temperature field of the steel particle-gasoline-air system at the ignition moment ( $\tau_d = 0.095$ ).

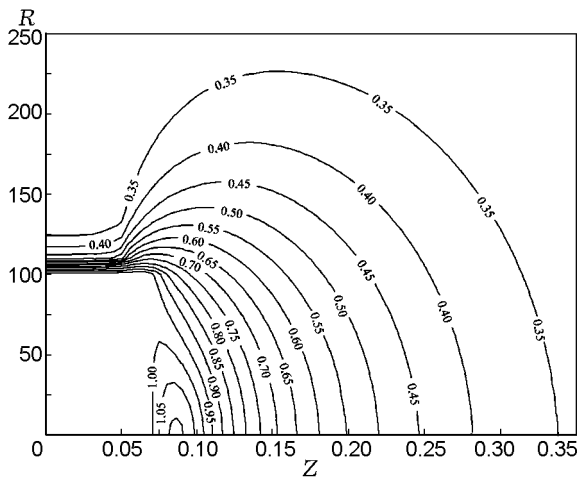


Fig. 4. Isotherms of the steel particle-gasoline-air system at the ignition moment ( $\tau_d = 0.095$ ).

der. Comparing the numerical values of  $\tau_d$  for ignition of a particle in the shape of a cylinder and a particle in the shape of a parallelepiped, it can be concluded that, with heat exchange conditions and liquid-particle contact areas being the same, the ignition delay is almost independent of the shape of the heating source. A similar conclusion was made in a study [22] of the interaction of hot particles with solid condensed substances. This result shows that two-dimensional models [6, 17] are suitable for the qualitative analysis of the examined process with heat sources in the shape of a parallelepiped of small sizes. This makes it possible to significantly simplify the computation and to exactly determine the main regularities of ignition in the system (see Fig. 1).

TABLE 2

Ignition Delay in the  
Steel Particle-Gasoline-Air System  
versus Particle Size and Shape for  $\Theta_{ch} = 1$

$H_{ch}$	$L_{ch}$	$\tau_d$
Particle in the shape of a parallelepiped (Fig. 1a)		
0.1	0.09	0.059
0.1	0.08	0.078
0.1	0.07	0.093
0.1	0.06	0.102
0.09	0.06	0.108
0.08	0.06	0.122
0.07	0.06	0.139
0.06	0.06	0.167
Particle in the shape of a cylinder (Fig. 1b)		
$R_{ch}$	$Z_{ch}$	$\tau_d$
0.1	0.09	0.063
0.1	0.08	0.084
0.1	0.07	0.095
0.1	0.06	0.107
0.09	0.06	0.112
0.08	0.06	0.124
0.07	0.06	0.142
0.06	0.06	0.169

At the same time, the small differences in the values of  $\tau_d$  for the examined particle shapes are due to the faster cooling of cylindrical particles compared to those having the shape of a parallelepiped and, as a consequence, to lower heat transfer to the ignition zone. It has been found [23] that, for the same characteristic sizes and similar heat-exchange conditions, the rate of temperature variation in time is maximal for spherical particles and minimal for particles in the shape of a parallelepiped. This is explained by the fact that the surface area to volume ratio, which is a determining factor for cooling and heating is the largest for a sphere. For bodies in the shape of a parallelepiped, this ratio is smaller than for a cylinder and a sphere. In the case of large particles ( $R_{ch} = Z_{ch} \geq 0.25$ ), this factor is more pronounced and the shape of the heating source should be taken into account. For  $R_{ch} = Z_{ch} < 0.25$  and  $\Theta_{ch} \geq 1$ , the effect of the particle shape on  $\tau_d$  can be ignored.

From Table 2, it is evident that the ignition delay decreases with increasing particle size, which, as in the case of increasing initial temperature  $\Theta_{ch}$ , is caused by an increase in the heat content of the ignition source. It should be noted that, as  $R_{ch}$  increases and  $Z_{ch}$  remains constant, the contact area between the particle

TABLE 3  
Ignition Delay in the  
Steel Particle–Gasoline–Air System  
versus Initial Mass Concentration  
of Water Vapor in the Air  $C_{m,w0}$   
for  $R_{ch} = 0.1$ ,  $Z_{ch} = 0.07$ , and  $\Theta_{ch} = 1$

$C_{m,w0}$	$\tau_d$
0	0.095
0.05	0.097
0.10	0.100
0.15	0.102
0.20	0.104
0.25	0.106
0.30	0.109
0.35	0.113
0.40	0.117
0.45	0.122
0.50	0.128

and liquid increases. This leads to expansion of the liquid heating zone, more intense vaporization, and an increase in the fuel concentration in the gas region. In the case of increasing  $Z_{ch}$  and constant  $R_{ch}$ , the contact area between the particle and air increases, resulting in an increase in the heat flow density in the ignition zone. Under such conditions, the ignition delay decreases sharply (see Table 2).

The effect of the air humidity on the delay of the examined process was studied (Table 3). Numerical analysis shows that at a rather low initial mass concentration of water vapor in air ( $C_{m,w0} \leq 0.2$ ), the ignition delay increases insignificantly compared to the case  $C_{m,w0} = 0$ . For  $C_{m,w0} > 0.2$ , the increase in the ignition delay with increasing humidity  $C_{m,w0}$  becomes more pronounced. For  $C_{m,w0} = 0.5$ , the deviations of the values of  $\tau_d$  from the same parameters for  $C_{m,w0} = 0$  exceed 20%. It is obvious that, at a high air humidity ( $C_{m,w0} \geq 0.5$ ) and relatively low particle temperatures ( $\Theta_{ch} < 0.8$ ), ignition does not occur in the examined system.

One more important factor should be noted. In papers on the ignition of substances in various states of aggregation [6–9, 17, 22], one commonly use the kinetic parameters  $k_0$  and  $E$  obtained in experiments in which heat sources were massive heated bodies. For single particles heated to high temperatures, these ignition parameters are currently unknown, which, in turn, can be explained by the absence of experimental data on these processes. In the present paper, we used the kinetic characteristics of gasoline obtained in experiments on ignition of its drops falling on the surface of a hot plate of large sizes [18].

In addition, experimental studies of ignition of typical liquid fuels have shown that even fuels of the same grade differ significantly in thermochemical and thermophysical properties [7]. This is true not only for liquid fuels but also of many widely used liquid fuels and further complicates experimental investigation of their ignition.

## CONCLUSIONS

The results show that the ignition mechanism of combustible liquids by single hot particles differs significantly from the same processes of solid condensed substances [9]. During ignition of liquids, the gas-phase ignition mechanism is pronounced. This is due to the fact that all liquids are ignited and burn in the gas phase. It can be concluded that the heterogeneous ignition mechanism [9] does not occur in liquids under any conditions.

From the results of the numerical analysis of the examined process, the liquid ignition characteristics in the examined formulation (see Fig. 2) are determined mainly by the heat content of the particles. An increase in the particle size leads to a reduction in the critical temperatures  $\Theta_{ch}$  at which ignition occurs. If the particle temperature increases considerably ( $\Theta_{ch} > 1.5$ ), ignition occurs even in the case of a heating source of small size ( $R_{ch} = Z_{ch} > 0.04$ ).

The numerical results suggest a high fire hazard of the process studied. At the same time, at high relative air humidity ( $\varphi_{12} > 0.50$ ) and relatively low temperatures of the heating source ( $\Theta_{ch} < 0.8$ ), ignition conditions of the vapor–gas mixture does not occur.

This work was supported by the Russian Foundation for Basic Research (Grant No. 06–08–00366-a).

## REFERENCES

1. V. I. Blinov and G. N. Khudyakov, *Diffusion Combustion of Liquids* [in Russian], Izd. Akad. Nauk SSSR (1961).
2. N. S. Khabeev and O. R. Ganiev, “Dynamics of a vapor shell around a heated particle in a liquid,” *Appl. Mech. Tech. Phys.*, **48**, No. 4, 525–533 (2007).
3. K. A. Avdeev, F. S. Frolov, and S. M. Frolov, “Nonstationary heat exchange of metal particles with gas,” *Khim. Fiz.*, **25**, No. 11, 17–24 (2006).
4. I. G. Namyatov, S. S. Minaev, V. S. Babkin, V. A. Bunev, and A. A. Korzhavin, “Diffusion combustion of a liquid fuel film on a metal substrate,” *Combust., Expl., Shock Waves*, **36**, No. 5, 562–570 (2000).
5. E. I. Gubin and I. G. Dik, “Spark ignition of atomized liquid fuel,” *Combust., Expl., Shock Waves*, **26**, No. 1, 8–11 (1990).

6. G. V. Kuznetsov and P. A. Strizhak, "Heat and mass transfer at the ignition of a liquid substance by a single hot particle," *J. Eng. Thermophys.*, No. 3, 244–252 (2008).
7. P. Dagaut and M. Cathonnet, "The ignition, oxidation, and combustion of kerosene: A review of experimental and kinetic modeling," *Prog. Energ. Combust. Sci.*, No. 32, 48–92 (2006).
8. F. A. Williams, *Combustion Theory* [in Russian], Addison-Wesley Pub., Reading (1985).
9. V. N. Vilyunov and V. E. Zarko, *Ignition of Solids*, Elsevier, Amsterdam (1989).
10. R. F. McAlevy, P. L. Cowan, and M. Summerfield, "The mechanism of ignition composite solid propellants by hot gases," in: M. Summerfield (ed.), *Progress in Astronautics and Rocketry*, Vol. 1: *Solid Propellant Rocket Research*, Academic Press, New York (1960).
11. P. J. Roach, *Computational Fluid Dynamics*, Hermosa, Albuquerque (1976).
12. D. A. Frank-Kamenetskii, *Diffusion and Heat Transfer in Chemical Kinetics*, Plenum, New York (1969).
13. Yu. V. Polezhaev and F. B. Yur'evich, *Thermal Protection* [in Russian], Énergiya, Moscow (1976).
14. V. P. Isachenko, *Heat Exchange during Condensation* [in Russian], Énergiya, Moscow (1977).
15. A. A. Samarskii, *Theory of Difference Schemes* [in Russian], Nauka, Moscow (1983).
16. L. A. Kozdoba, *Methods of Solution of Nonlinear Heat-Conduction Problems* [in Russian], Nauka, Moscow (1975).
17. G. V. Kuznetsov and P. A. Strizhak, "Ignition of liquid hydrocarbon fuels by a heated single particle," *Izv. Tomsk Politekh. Unhiv.*, No. 4, 5–9 (2008).
18. E. S. Shchetinkov, *Physics of Gas Combustion* [in Russian], Nauka, Moscow (1965).
19. N. B. Vargaftik, *Handbook on Thermophysical Properties of Gases and Liquids* [in Russian], Stars, Moscow (2006).
20. V. N. Yureneva and P. D. Lebedeva, *Heat Engineering Handbook* [in Russian], Vol. 1, Énergiya, Moscow (1975).
21. V. N. Yureneva and P. D. Lebedeva, *Heat Engineering Handbook* [in Russian], Vol. 2, Énergiya, Moscow (1975).
22. G. V. Taratushkina, "Heat and mass transfer during ignition of condensed substances and erosion of structural materials during inertial sedimentation of hot solid particles," Candidate Dissertation in Phys.-Math. Sci., Tomsk (2004).
23. A. V. Lykov and Yu. A. Mikhailov, *Theory of Heat and Mass Transfer* [in Russian], Gosénergoizdat, Leningrad (1963).